

Bacteria inactivation by sulfate radical: progress and non-negligible disinfection by-products

Xin Zhou^{1,2}, Xiaoya Ren^{1,2}, Yu Chen^{1,2}, Haopeng Feng^{1,2}, Jiangfang Yu^{1,2}, Kang Peng^{1,2}, Yuying Zhang^{1,2},
Wenhao Chen^{1,2}, Jing Tang^{1,2}, Jiajia Wang (✉)^{1,2}, Lin Tang (✉)^{1,2}

¹ College of Environmental Science and Engineering, Hunan University, Changsha 410082, China

² Key Laboratory of Environmental Biology and Pollution Control (Hunan University), Ministry of Education, Changsha 410082, China

HIGHLIGHTS

- Status of inactivation of pathogenic microorganisms by $\text{SO}_4^{\cdot-}$ is reviewed.
- Mechanism of $\text{SO}_4^{\cdot-}$ disinfection is outlined.
- Possible generation of DBPs during disinfection using $\text{SO}_4^{\cdot-}$ is discussed.
- Possible problems and challenges of using $\text{SO}_4^{\cdot-}$ for disinfection are presented.

ARTICLE INFO

Article history:

Received 29 May 2022

Revised 19 August 2022

Accepted 22 August 2022

Available online 30 September 2022

Keywords:

Sulfate radicals

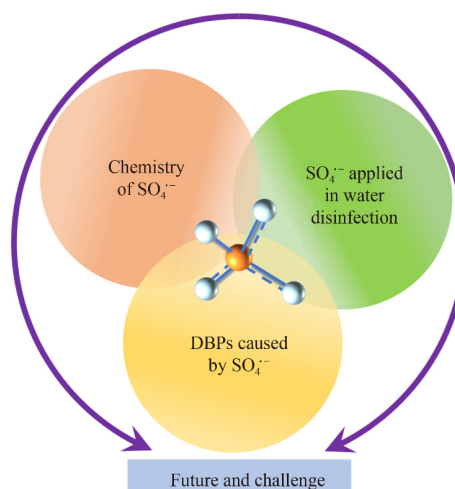
Disinfection by-products

Inactivation mechanisms

Bacterial inactivation

Water disinfection

GRAPHIC ABSTRACT



ABSTRACT

Sulfate radicals have been increasingly used for the pathogen inactivation due to their strong redox ability and high selectivity for electron-rich species in the last decade. The application of sulfate radicals in water disinfection has become a very promising technology. However, there is currently a lack of reviews of sulfate radicals inactivated pathogenic microorganisms. At the same time, less attention has been paid to disinfection by-products produced by the use of sulfate radicals to inactivate microorganisms. This paper begins with a brief overview of sulfate radicals' properties. Then, the progress in water disinfection by sulfate radicals is summarized. The mechanism and inactivation kinetics of inactivating microorganisms are briefly described. After that, the disinfection by-products produced by reactions of sulfate radicals with chlorine, bromine, iodide ions and organic halogens in water are also discussed. In response to these possible challenges, this article concludes with some specific solutions and future research directions.

© The Author(s) 2022. This article is published with open access at link.springer.com and journal.hep.com.cn

1 Introduction

Disinfecting is an important process to eliminate

microorganism, pathogenic bacteria and other biological hazards (Anipsitakis et al., 2008; Xiao et al., 2019; Lei et al., 2021). Chlorination as the most used disinfection method commonly results in disinfection by-products (DBPs) and may be noneffective against resistant microorganisms (Wang et al., 2019; Wang et al., 2021; Liang et al., 2022; Zhao et al., 2022). In this case, current

✉ Corresponding authors

E-mails: wangjiajia07@hnu.edu.cn (J. Wang);

tanglin@hnu.edu.cn (L. Tang)

research focus has shifted to using reactive oxygen species (such as hydroxyl radicals, singlet oxygen, sulfate radicals, and superoxide radicals) which generated in advanced oxidation processes (AOPs) to degrade pollutants and inactivate pathogens due to their high redox potential (Zhang et al., 2010; Sun et al., 2016; Wang et al., 2017a; Wang et al., 2018; Yu et al., 2020). For example, Bai et al. (2022) explored the mechanism of superoxide radical ($O_2^{\bullet-}$) degradation of perfluorocarboxylic acid (PFCAs). The results revealed that the low polar solvent enhanced the nucleophilicity of $O_2^{\bullet-}$, but also reduced the desolvation process of PFCAs, leading to a decrease in kinetics. Cho et al. (2004) studied photocatalytic inactivation of bacteria with TiO_2 , and found that the amount of hydroxyl radicals ($\bullet OH$) has an excellent linear relationship with the degree of *E. coli* inactivation under constant temperature. Current research has demonstrated that generation of large amounts of $\bullet OH$ in Fenton's reaction requires a strictly acidic environment (pH 2–4) (Pignatello et al., 2006; Tang et al., 2022). Therefore, the practical application of Fenton's reaction in disinfection is extremely limited.

At present, sulfate radical ($SO_4^{\bullet-}$) was found to be a perfect substitution to $\bullet OH$ as its abilities in irreversibly destroying cell structure or function (Zhang et al., 2014; Sun et al., 2016; Xiao et al., 2020). $SO_4^{\bullet-}$ is generated by persulfate (PS) or peroxymonosulfate (PMS). Compared with hydrogen peroxide (H_2O_2) that forms $\bullet OH$, solid PMS and PS are cheaper, more stable, and more convenient to store and transport (Waclawek et al., 2017). Meanwhile, $SO_4^{\bullet-}$ can selectively oxidize biomolecules and macromolecules with electron-rich groups, making it more suitable for inactivating microorganisms (Neta et al., 1988). There are more and more researches on sulfate radicals-based AOPs (SR-AOPs) in water disinfection in recent years, and promising results have been achieved (Rodríguez-Chueca et al., 2017b; Wen et al., 2017; Marjanovic et al., 2018; Zhou et al., 2018; Wu et al., 2019; Ferreira et al., 2020; Wang et al., 2020a). For example, Zhang et al. (2020) investigated the effect of sulfidated micron zero-valent iron/PS (S-mZVI/PS) system on the viability of inactivating *E. coli*. The results showed that 7–8 log *E. coli* was completely eliminated within 30 minutes after treated with 1 mmol/L PS and 40 mg/L S-mZVI.

Unfortunately, as a strong oxidant similar to $\bullet OH$, $SO_4^{\bullet-}$ may react with halogen ions in water during disinfection to produce DBPs which can cause bladder cancer, colorectal cancer, miscarriage and birth defects (including heart defects found in 2016) (Richardson and Kimura, 2019). Fang and Shang (2012) firstly discovered that $SO_4^{\bullet-}$ can oxidize bromide (Br^-) to cancerogen bromate (BrO_3^-). Later, Lu et al. (2015) studied the conversion of bromide in the heat activated oxidation process of PS in the presence of humic acid (HA) and confirmed the formation of bromoform and bromoacetic

acid. Under acidic conditions, chloride (Cl^-) has a similar conversion process in the UV/PS process, and $SO_4^{\bullet-}$ can also convert Cl^- into chlorate (ClO_3^-) which is harmful to humans (Lutze et al., 2015). Many studies use SR-AOPs for disinfection and sterilization without discussing the risks of generating DBPs which can not be ignored. Accordingly, based on the prospect and existing problems of sulfate radicals in the disinfection process, they are more suitable for the disinfection of aquaculture, swimming pool and ballast water.

Previous reviews on the topic of SR-AOPs in water disinfection, mainly focused on high-efficiency inactivation in the process, but few of them considered the impact of subsequent DBPs. Therefore, this review has mainly done the following work: 1) Briefly summarized the properties of sulfate radical; 2) Comprehensively reviewed the research on sulfate radical inactivation; 3) Discussed the possible formation of DBPs in the process; 4) Stated possible existence problems and future challenges.

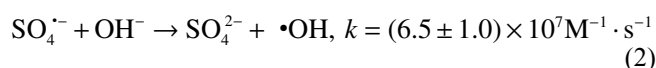
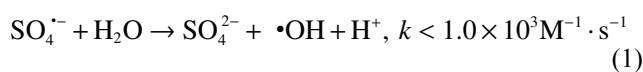
2 Chemistry of sulfate radical

Table 1 lists the oxidation potentials of oxidants commonly used in water treatment. As displayed in the table, $SO_4^{\bullet-}$ is a strong oxidant with a standard redox potential of 2.5–3.1 V vs. NHE (normal hydrogen electrode), which is close to $\bullet OH$ (+2.80 V vs. NHE) (Lian et al., 2017). The half-life of the $SO_4^{\bullet-}$ is 30–40 μs , which is longer than $\bullet OH$ (10^{-3} μs) (Devasagayam et al., 2004). At the same time, $SO_4^{\bullet-}$ tends to react with organic matter in the process of electron transfer, while $\bullet OH$ participates in various reactions without selectivity (Ghanbari and Moradi, 2017). This means that $SO_4^{\bullet-}$ are more selective than $\bullet OH$. Since sulfate radical is electrophilic, it prefers to react with electron-donating groups rather than electron-withdrawing groups (Hu and

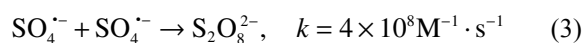
Table 1 Oxidation potentials of oxidants commonly used in water

Oxidant	Oxidation potential (V)	Ref.
Fluorine	3.0	Guerra-Rodríguez et al., 2018
Hydroxyl radical	2.8	Wang and Wang, 2018
Sulfate radical	2.5–3.1	Ferreira et al., 2020
Ozone	2.1	Ao et al., 2021
Persulfate	2.0	Waclawek et al., 2017
Peracetic acid (PAA)	1.96	Ao et al., 2021
Peroxymonosulfate	1.8	Ao et al., 2021
H_2O_2	1.8	Ao et al., 2021
Potassium permanganate	1.7	Ao et al., 2021
Chlorine dioxide	1.5	Ao et al., 2021
Chlorine	1.4	Ao et al., 2021

Long, 2016). Generally, the reaction between $\text{SO}_4^{\bullet-}$ and organic molecules is very fast and the second-order rate constant is between 10^5 to $10^9 \text{ M}^{-1} \cdot \text{s}^{-1}$ (Neta et al., 1988; Oh et al., 2016). Sulfate radicals can react effectively with organic compounds with the similar reactivity in the pH range of 2–8 (Oh et al., 2016). In addition, the radicals can also react with water to generate $\bullet\text{OH}$, and the reaction equation is as follows (Eqs. (1) and (2)) (Waldemer et al., 2007):



Equations (1) and (2) can occur at all pH conditions, but under alkaline conditions, the reaction of Eq. (2) is more pronounced. When $\text{pH} > 8.5$, $\text{SO}_4^{\bullet-}$ is rapidly decomposed into $\bullet\text{OH}$, and when $\text{pH} > 10.7$, $\bullet\text{OH}$ becomes the dominant radical (Yang et al., 2010). In addition, the $\text{SO}_4^{\bullet-}$ can react with themselves (Eq. (3)) (Huie and Clifton, 1993). Due to the low concentration of $\text{SO}_4^{\bullet-}$, its self-scavenging effect can be ignored.



3 Sulfate radical applied in water disinfection

Sulfate radical is mainly produced by PS and PMS activation. Moreover, the essential mechanism of PS and PMS activation is the O–O bond fracture in their structures (Wang and Wang, 2018). PS is easier to be activated than PMS, because the O–O bond of PS (0.149 nm) is longer than that of PMS (0.146 nm) (Hu et al., 2020). There are many activation methods, such as heat, UV, base, transient metals and carbon-based materials (Lei et al., 2015; Xiao et al., 2018). The effectiveness of SR-AOPs in degrading organic pollutants has been proven. In recent years, this technology has been applied to inactivate microorganisms and has exhibited good performance. It is considered as a valuable and promising technology in water disinfection.

3.1 Mechanisms for water disinfection

At present, the literature on $\text{SO}_4^{\bullet-}$ inactivating microorganisms is relatively limited, and the inactivation mechanism remains to be further studied. Wen et al. (2017) explored the inactivation mechanism of four fungal spores under UV and UV/PMS systems. Unlike the results of UV irradiation alone, when PMS was added to the system, the appearance of large amounts of DNA was detected outside the cells. They analyzed the cell morphology of the four fungi before and after the reaction (Fig. 1(a)). The results showed that in the presence of

PMS, the spore structure was disrupted and the cell wall was significantly damaged. So far, the inactivate microorganisms with $\text{SO}_4^{\bullet-}$ are mainly explained by the destruction of cell membranes/cell walls, enzymes and genetic material (Xiao et al., 2019). The inactivation mechanism is illustrated in Fig. 1(b).

The process of microorganism inactivation is that $\text{SO}_4^{\bullet-}$ first modify bacterial cell membranes and cell walls to change their permeability, which accelerates the penetration of oxidants, and then destroy intracellular components. Subramanian et al. (2013) and Wang et al. (2020a) used agarose gel electrophoresis to prove that $\text{SO}_4^{\bullet-}$ damage genetic material. Studies have found that, certain components of microorganisms such as guanine are more likely to react with $\text{SO}_4^{\bullet-}$ instead of $\bullet\text{OH}$ (Roginskaya et al., 2016). In addition, the chain scission rate caused by $\text{SO}_4^{\bullet-}$ is much higher than that by $\bullet\text{OH}$ (Sonntag, 2006), which means that $\text{SO}_4^{\bullet-}$ cause more serious damage to DNA than $\bullet\text{OH}$. Although Zhang et al. (2020) have found that the $\text{SO}_4^{\bullet-}$ disinfection system has a lipid peroxidation effect on cell membranes, due to the existence of symbiotic $\bullet\text{OH}$, the lipid peroxidation effect of $\text{SO}_4^{\bullet-}$ alone needs to be further confirmed. In terms of protein oxidation, $\text{SO}_4^{\bullet-}$ can cause protein cross-linking (Fancy and Kodadek, 1999), attack the carboxyl groups in amino acids (Davies et al., 1984), and initiate free radical chain reactions. Gau et al. (2010) compared the oxidation of protein by $\text{SO}_4^{\bullet-}$ and $\bullet\text{OH}$, and found that the modification and residue selectivity of the two were very similar. As a consequence, it can be roughly inferred that the process of inactivating microorganisms by $\text{SO}_4^{\bullet-}$ and $\bullet\text{OH}$ is similar. It seems that $\text{SO}_4^{\bullet-}$ can also penetrate into cells and cause intracellular reactive oxygen species (ROS) to continuously increase and cause cell death. However, the mechanism of $\text{SO}_4^{\bullet-}$ inactivating microorganisms needs further investigation.

3.2 Inactivation kinetics

The inactivation studies of *E. coli*, other bacteria and some fungi by SR-AOPs are summarized in Tables 2–4. It can be seen that different activation methods have different inactivation efficiency for microorganisms. Among them, the most studied subjects are UV activations of PS and PMS to produce $\text{SO}_4^{\bullet-}$ for water disinfection and inactivation of microorganisms, followed by transition metal activation. As we can see, iron is the most commonly used transition metals, followed by cobalt. The widely studied target microorganism is *E. coli*, regarded as an indicator of fecal pollution in aquatic environments (Xiao et al., 2020). Furthermore, it is easy to obtain and cultivate, and its structure and composition are representative (Qi et al., 2020). In addition, the inactivation of viruses, fungi and other bacteria such as *S. aureus*, *E. faecalis* and *B. mycoides* has also been studied.

Venieri et al. (2020) explored the inactivation effect of

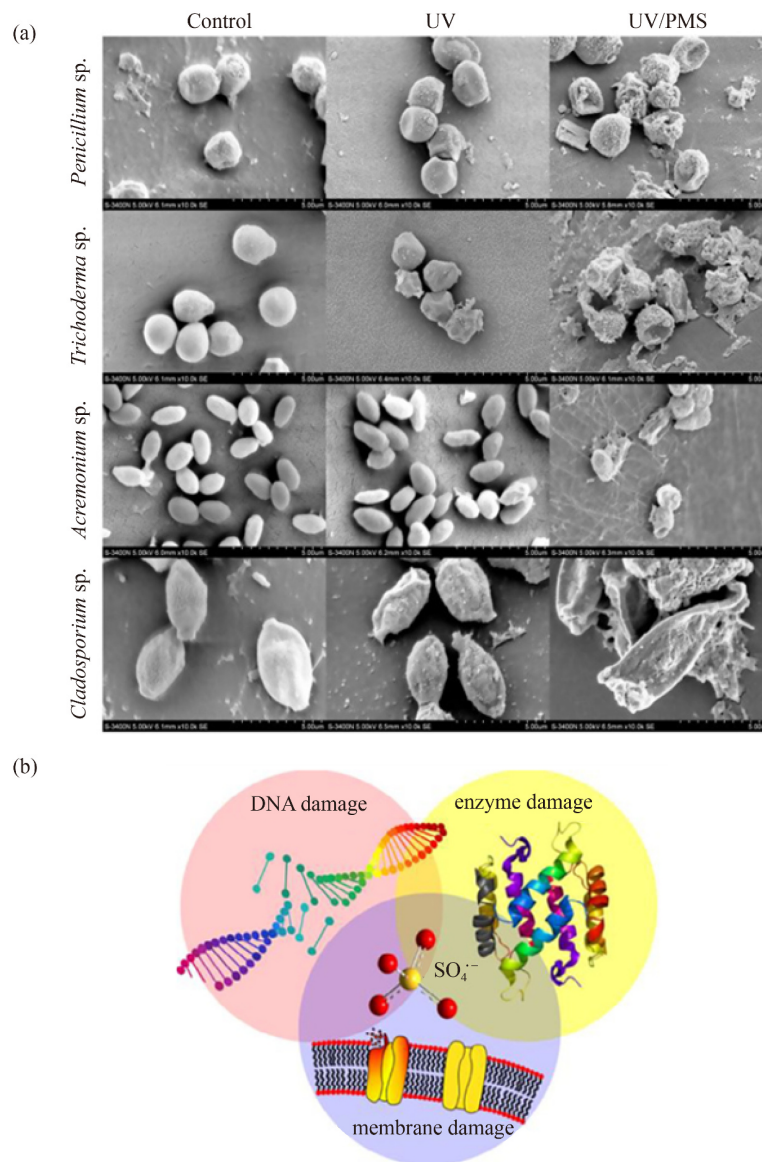


Fig. 1 (a) SEM images of fungal spores before and after treatment (control (left), UV (middle) and UV/PMS (right)). Experimental conditions: UV=40 mJ/cm², PMS=0.1 mmol/L, spore concentration=10⁷ CFU/mL (Wen et al., 2017) (Copyright 2017 Elsevier, Reprinted with permission from Elsevier); (b) mechanism of inactivation of bacteria by sulfate radicals (Xiao et al., 2019) (Copyright 2019 Elsevier, Reprinted with permission from Elsevier).

UVA/PS on *E. coli* and found that 300 mg/L PS can inactivate 6 log of *E. coli* after UVA irradiation for 180 min. Rodríguez-Chueca et al. (2017b) investigated the inactivation efficiency of several bacteria by PMS under UV-A LED and fitted their inactivation kinetics. They found that Hom's model fits all results of bacterial inactivation. They also discovered that in the UV-A LED/PMS system, the Hom's kinetic rate constant of *E. coli* was the largest at 0.39 min⁻¹, followed by *S. aureus* (0.33 min⁻¹), and finally *B. mycoides* (0.06 min⁻¹). It may be explained by that the different structures of different bacteria lead to the difference of inactivation kinetic constants.

To control disinfection costs, Wang et al. (2019) explored the feasibility of sunlight /PS water disinfection.

The results showed that VL/PS had a certain inactivation efficiency for bacteria (7 log reduction for *S. aureus*, *E. coli* and *P. aeruginosa*, after 200 min, 120 min and 140 min of VL irradiation with a PS dose of 2 mg/L, respectively). In their experiments, the log-linear-shoulder model was applied to fit the inactivation kinetics of VL/PS, thermal/PS, and VL/thermal/PS, and they found kinetic constants for these three systems to be 0.25 min⁻¹, 0.38 min⁻¹, and 1.29 min⁻¹, respectively. It can be concluded that the increase in temperature caused by sunlight exposure will further accelerate the process of bacterial inactivation. They also explored the effect of PS on the inactivation efficiency of *E. coli*, and found that the inactivation rate constant increased with the increase

Table 2 Summary of *E.coli* inactivation by SR-AOPs

Microorganisms	Initial conc. (CFU/mL)	System	Max. Log removal value	Dosage	Exposure time (min)	Ref.
<i>E. coli</i>	10 ⁵	g-C ₃ N ₄ /VL/PMS	5	g-C ₃ N ₄ 0.1 g/L PMS 0.5 mmol/L	120	Zhang et al., 2021
<i>E. coli</i>	10 ⁸	VL/PS/MHC	8	MHC 200 mg/L PS 2 mmol/L	40	Wang et al., 2020a
<i>E. coli</i>	10 ⁷	UVA-LED/PMS	5.9	PMS 1 mg/L	60	Qi et al., 2020
<i>E. coli</i>	10 ⁶	Fe ³⁺ /PS	6	PS 200 mg/L Fe ³⁺ 30 mg/L	15	Venieri et al., 2020
<i>E. coli</i>	10 ⁶	50 °C/PS	6	PS 100 mg/L	60	Venieri et al., 2020
<i>E. coli</i>	10 ⁶	UVA/PS	6	PS 300 mg/L	180	Venieri et al., 2020
<i>E. coli</i>	10 ⁶	US/PS	6	PS 100 mg/L	120	Venieri et al., 2020
<i>E. coli</i>	10 ⁶	PS/solar	6	PS 0.5 mmol/L	20	Ferreira et al., 2020
<i>E. coli</i>	10 ⁶	US/Ag-BTO/PS	6.2	Ag-BTO ₂ mg/mL PS 1 mmol/L	5 20(VBNC)	Xia et al., 2020
<i>E. coli</i>	10 ⁷	CINMs/PMS	7	PMS 0.1 mmol/L	1	Shan et al., 2020
<i>E. coli</i>	10 ⁷ to 10 ⁸	S-mZVI/PS	completely eliminated	S-mZVI 40 mg/L PS 1 mmol/L	30	Zhang et al., 2020
<i>E. coli</i>	10 ⁶	CoFe ₂ O ₄ /PMS/UVA	6	CoFe ₂ O ₄ 0.05 g/L PMS 0.2 mmol/L	30	Rodríguez-Chueca et al., 2020
<i>E. coli</i>	10 ⁷	VL/PS	7	PS 2 mmol/L	120	Wang et al., 2019
<i>E. coli</i>	10 ⁷ to 10 ⁸	3D-GFP	4.6	Na ₂ SO ₄ 50 mmol/L PS 2 mmol/L	10	Ma et al., 2019
<i>E. coli</i>	10 ⁶	sunlight/Fe ²⁺ /40 °C/PMS	6	1 mg/L Fe ²⁺ 1.8×10 ⁻⁵ mol/L PMS	30	Rodríguez-Chueca et al., 2019a
<i>E. coli</i>	10 ⁵	PMS/UVA	5	1 mmol/L PMS	30	Rodríguez-Chueca et al., 2019b
<i>E. coli</i>	10 ⁵	PS/ Fe ²⁺ /UVA	5	0.5 mmol/L PS 1 mg/L Fe ²⁺	2	Rodríguez-Chueca et al., 2019b
<i>E. coli</i>	10 ⁷	PS/hv/ tris(2,2'-bipyridyl) ruthenium(II)	7	PS 2 mmol/L tris(2,2'-bipyridyl) ruthenium(II) 1 μmol/L	90	Subramanian et al., 2013
<i>E. coli</i>	9.2×10 ⁵	PS/UV	3	PS 10 mg/L	5	Michael-Kordatou et al., 2015
<i>E. coli</i>	10 ⁵	solar/PS/Fe ²⁺	3	PS 150 mg/L Fe ²⁺ 5 mg/L	60	Garkusheva et al., 2017
<i>E. coli</i>	10 ³ to 10 ⁴	UVA/PMS/Fe ²⁺	4.2	0.1 mmol/L PMS 0.1 mmol/L Fe ²⁺	120	Rodríguez-Chueca et al., 2017a
<i>E. coli</i>	10 ³ to 10 ⁴	UVA/PMS/Co ²⁺	3.2	0.1 mmol/L PMS 0.1 mmol/L Co ²⁺	120	Rodríguez-Chueca et al., 2017a
<i>E. coli</i>	10 ³ to 10 ⁴	UVA/PMS/Fe ²⁺	6.5	0.1 mmol/L PMS 0.1 mmol/L Fe ²⁺	30	Rodríguez-Chueca et al., 2017b
<i>E. coli</i>	10 ³ to 10 ⁴	UVA/PMS/Co ²⁺	6.5	0.1 mmol/L PMS 0.1 mmol/L Co ²⁺	60	Rodríguez-Chueca et al., 2017b
<i>E. coli</i>	10 ⁷	NP/PS	7	PS 1 mmol/L NP 1.25 g/L	20	Xia et al., 2017
<i>E. coli</i>	10 ⁵	Ilmenite/PS/VL	7	Ilmenite 1g/L PS 0.5 mmol/L	20	Xia et al., 2018
<i>E. coli</i>	10 ⁷	Single-atom Ru/PMS		Single-atom Ru 40 mg/L PMS 5 mg/L	1.5	Zhou et al., 2022
ARB <i>E. coli</i>	10 ⁷	PS(PMS)/O ₃	2	PS(PMS) 1 mg/L O ₃ 3 mg/L	10	Xiao et al., 2020

of PS. This is mainly due to the increase of sulfate radical. However, high concentrations of PS may also negatively affect the inactivation efficiency. This is mainly because excessive PS will quench SO₄^{•-} (Eqs. (4) and (5)), resulting in the formation of a critical PS concentration (Moreno-Andrés et al., 2019). For example, Venieri et al. (2020) showed that for the Fe²⁺/PS system,

the inactivation efficiency first increased with the increase of PS concentration, while the inactivation efficiency decreased instead when the PS concentration increased from 0.8 mmol/L to 1.3 mmol/L. Later, Wang et al. (2020a) introduced magnetic hydrochar (MHC) into the VL/PS system, and the results showed that the introduction of MHC enhances the inactivation rate

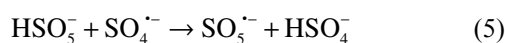
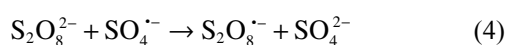
Table 3 Summary of inactivation of other bacteria by SR-AOPs

Microorganisms	Initial conc. (CFU/mL)	System	Max. Log removal value	Dosage	Exposure time (min)	Ref.
<i>E. faecalis</i>	10 ⁶	Fe ³⁺ /PS	6	PS 200 mg/L Fe ³⁺ 30 mg/L	15	Venieri et al., 2020
<i>E. faecalis</i>	10 ⁶	50 °C/PS	2.5	PS 100 mg/L	180	Venieri et al., 2020
<i>E. faecalis</i>	10 ⁶	UVA/PS	6	PS 300 mg/L	180	Venieri et al., 2020
<i>E. faecalis</i>	10 ⁶	US/PS	6	PS 200 mg/L	120	Venieri et al., 2020
<i>E. faecalis</i>	10 ⁷	ZVI/PS	6	PS 1 mmol/L ZVI 0.2 g/L	12	Liu et al., 2020
<i>E. faecalis</i>	10 ⁶	PS/solar	6	PS 0.7 mmol/L	20	Ferreira et al., 2020
<i>E. faecalis</i>	10 ⁶	solar/PS/ Fe(III)EDDS	5.6	PS 0.5 mmol/L Fe(III)EDDS 0.1 mmol/L	210	Bianco et al., 2017
<i>B. subtilis</i>	10 ⁷	tris(2,2'-bipyridyl) ruthenium(II)/PS/hv	7	PS 2 mmol/L tris(2,2'-bipyridyl) ruthenium(II) 1 µmol/L	90	Subramanian et al., 2013
<i>B. subtilis</i>	10 ⁶ to 10 ⁸	PS/UV	4.1	PS 30 mmol/L	60	Sabeti et al., 2017
<i>B. mycooides</i>	10 ³ to 10 ⁴	UVA/PMS	2.82	0.1 mmol/L PMS	120	Rodríguez-Chueca et al., 2017a
<i>B. mycooides</i>	10 ³ to 10 ⁴	UVA/PMS/Fe ²⁺	2.51	0.1 mmol/L PMS 0.1 mmol/L Fe ²⁺	90	Rodríguez-Chueca et al., 2017a
<i>B. mycooides</i>	10 ³ to 10 ⁴	UVA/PMS/Co ²⁺	1.71	0.1 mmol/L PMS 0.1 mmol/L Co ²⁺	90	Rodríguez-Chueca et al., 2017a
<i>B. mycooides</i>	10 ³ to 10 ⁴	UVA/PMS/Co ²⁺	3.4	0.1 mmol/L PMS 0.1 mmol/L Co ²⁺	120	Rodríguez-Chueca et al., 2017b
<i>B. mycooides</i>	10 ³ to 10 ⁴	UVA/PMS/Fe ²⁺	3.2	0.1 mmol/L PMS 0.1 mmol/L Fe ²⁺	30	Rodríguez-Chueca et al., 2017b
<i>S. aureus</i>	10 ⁸	VL/PS/MHC	8	MHC 200 mg/L PS 2 mmol/L	120	Wang et al., 2020a
<i>S. aureus</i>	10 ⁷	CINMs/PMS	7	PMS 0.2 mmol/L	3	Shan et al., 2020
<i>S. aureus</i>	10 ⁷	VL/PS	7	PS 2 mmol/L	200	Wang et al., 2019
<i>S. aureus</i>	10 ⁷	tris(2,2'-bipyridyl) ruthenium(II)/PS/hv	7	PS 2 mmol/L tris(2,2'-bipyridyl) ruthenium(II) 1 µmol/L	60	Subramanian et al., 2013
<i>S. aureus</i>	10 ³ to 10 ⁴	UVA/PMS	4.02	0.1 mmol/L PMS	120	Rodríguez-Chueca et al., 2017a
<i>S. aureus</i>	10 ³ to 10 ⁴	UVA/PMS/Co ²⁺	3.14	0.1 mmol/L PMS 0.1 mmol/L Co ²⁺	120	Rodríguez-Chueca et al., 2017a
<i>S. aureus</i>	10 ³ to 10 ⁴	UVA/PMS/Fe ²⁺	2.84	0.1 mmol/L PMS 0.1 mmol/L Fe ²⁺	120	Rodríguez-Chueca et al., 2017a
<i>S. aureus</i>	10 ³ to 10 ⁴	UVA/PMS/Co ²⁺	6.1	0.1 mmol/L PMS 0.1 mmol/L Co ²⁺	120	Rodríguez-Chueca et al., 2017b
<i>S. aureus</i>	10 ³ to 10 ⁴	UVA/PMS/Fe ²⁺	3.2	0.1 mmol/L PMS 0.1 mmol/L Fe ²⁺	120	Rodríguez-Chueca et al., 2017b
<i>S. aureus</i>	10 ⁷	NP/PS	7	PS 1 mmol/L NP 1.25 g/L	20	Xia et al., 2017
<i>P. aeruginosa</i>	10 ⁸	VL/PS/MHC	8	MHC 200 mg/L PS 2 mmol/L	60	Wang et al., 2020a
<i>P. aeruginosa</i>	10 ⁷	Cu(II)/PMS	3.4	Cu(II) 5 µmol/L PMS 0.2 mmol/L	20	Lee et al., 2020
<i>P. aeruginosa</i>	10 ⁷	Cu(II)/PMS/Cl ⁻	3.1	Cu(II) 5 µmol/L PMS 0.2 mmol/L NaCl 10 mmol/L	10	Lee et al., 2020
<i>P. aeruginosa</i>	10 ⁷	VL/PS	7	PS 2 mmol/L	140	Wang et al., 2019
<i>P. aeruginosa</i>	10 ⁷	tris(2,2'-bipyridyl) ruthenium(II)/PS/hv	7	PS 2 mmol/L tris(2,2'-bipyridyl) ruthenium(II) 1 µmol/L	120	Subramanian et al., 2013
ARB <i>pseudomonas</i> sp.	10 ⁸	UVC/PMS	5.3	PMS 1 mg/L	10	Hu et al., 2019b
<i>Enterococcus</i> sp.	10 ⁶	CoFe ₂ O ₄ /PMS/UVA	6	CoFe ₂ O ₄ 0.05 g/L PMS 0.2 mmol/L	45	Rodríguez-Chueca et al., 2020
<i>Enterococcus</i> sp.	10 ⁶	PMS/UVA	6	PMS 1 mmol/L	90	Rodríguez-Chueca et al., 2019b

Table 4 Summary of fungus inactivation by SR-AOPs

Microorganisms	Initial conc. (CFU/mL)	System	Max. Log removal value	Dosage	Exposure time (min)	Ref.
<i>C. albicans</i>	10 ³ to 10 ⁴	UVA/PMS	4.67	10 mmol/L PMS	15	Rodríguez-Chueca et al., 2017a
<i>C. albicans</i>	10 ³ to 10 ⁴	UVA/PMS/Fe ²⁺	1.41	10 mmol/L PMS 5 mmol/L Fe ²⁺	15	Rodríguez-Chueca et al., 2017a
<i>C. albicans</i>	10 ³ to 10 ⁴	UVA/PMS/Co ²⁺	3.64	10 mmol/L PMS 5 mmol/L Co ²⁺	15	Rodríguez-Chueca et al., 2017a
<i>C. albicans</i>	10 ³ to 10 ⁴	UVA/PMS/Co ²⁺	5.3	5 mmol/L PMS 2.5 mmol/L Co ²⁺	30	Rodríguez-Chueca et al., 2017b
<i>C. albicans</i>	10 ³ to 10 ⁴	UVA/PMS/Fe ²⁺	5	5 mmol/L PMS 2.5 mmol/L Fe ²⁺	60	Rodríguez-Chueca et al., 2017b
<i>Acremonium</i> sp.	(2–7)×10 ⁵	PMS/UV	5	PMS 0.1 mmol/L	6	Wen et al., 2017
<i>Acremonium</i> sp.	(2–7)×10 ⁵	PS/UV	3.7	PS 0.1 mmol/L	6	Wen et al., 2017
<i>Cladosporium</i> sp.	(2–7)×10 ⁵	PMS/UV	4.9	PMS 0.1 mmol/L	15	Wen et al., 2017
<i>Cladosporium</i> sp.	(2–7)×10 ⁵	PS/UV	3.9	PS 0.1 mmol/L	15	Wen et al., 2017
<i>Penicillium</i> sp.	(2–7)×10 ⁵	PMS/UV	6.2	PMS 0.1 mmol/L	9	Wen et al., 2017
<i>Penicillium</i> sp.	(2–7)×10 ⁵	PS/UV	5.9	PS 0.1 mmol/L	9	Wen et al., 2017
<i>Trichoderma</i> sp.	(2–7)×10 ⁵	PMS/UV	5.2	PMS 0.1 mmol/L	6	Wen et al., 2017
<i>Trichoderma</i> sp.	(2–7)×10 ⁵	PS/UV	5	PS 0.1 mmol/L	6	Wen et al., 2017

constant (k). *E. coli* in 8 log quantities were totally inactivated within 40 minutes. The k value increased from 0.19 min⁻¹ in PS/MHC system to 0.99 min⁻¹ in PS/MHC/VL system, and the inactivation efficiency increased by 5.21 times. The quenching experiments and EPR results showed that sulfate radical was the main free radical in PS/MHC and PS/MHC/VL systems. Moreover, the introduction of MHC led to a large increase in the concentration of sulfate radical and ultimately enhanced the inactivation efficiency.

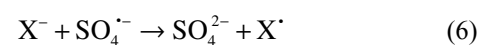


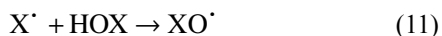
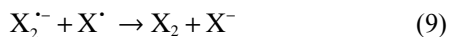
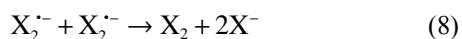
Xiao et al. (2020) explored the inactivation kinetics of *E. faecalis* and *E. coli* by using zero-valent iron to activate PS. The pseudo-first-order inactivation rates for *E. faecalis* and *E. coli* to be 0.0924 min⁻¹ and 0.0304 min⁻¹, respectively. In addition, they measured a second-order rate constant of (1.29–1.49)×10⁹ M⁻¹·s⁻¹ for *E. coli* and (6.61–6.81)×10⁹ M⁻¹·s⁻¹ for *E. faecalis*. The results showed that the inactivation effect of SO₄^{•-} on Gram-positive bacterium was better than that of Gram-negative bacterium. Rodríguez-Chueca et al. (2019b) assessed the bacterial inactivation effect of homogeneous and heterogeneous Fe systems upon activation of PMS and PS under UV-A radiation. The experimental results showed that PMS system had better inactivation effect on bacteria than the PS system. Moreover, different Fe species had different inactivation effects on *E. coli* and *Enterococcus* sp. Among them, Fe(III)-citrate has a positive impact on the inactivation kinetics of *Enterococcus* sp. due to the production of additional oxidizing species such as superoxide radicals and hydrogen peroxide. In the heterogeneous system, compared with Fe₃O₄, nano-zero

valent iron has inactivation effect on both bacteria, which is a very promising treatment method. In addition, some researchers have also explored the inactivation effects of magnetic pyrrhotite/PS (NP/PS) (Xia et al., 2017), S-mZVI/PS (Zhang et al., 2020) and CoFe₂O₄/PMS/UVA (Rodríguez-Chueca et al., 2020) systems on *E. coli*. The results show that these complex systems have enhancement of microorganism inactivation.

4 DBPs caused by SR-AOPs in water disinfection

As an economical and effective technique, SR-AOPs have received increasing attention in microorganisms inactivation. However, SO₄^{•-} will react with halide ions and convert them to reactive halogen species (RHS), which can be further oxidized to chlorates and bromates by the SO₄^{•-}. RHS can also react with natural organic matter (NOM) and halogenated organic pollutants to form halogenated DBPs (Xie et al., 2016; Zhang et al., 2019). The conversion mechanism of halide ions when it coexists with SO₄^{•-} is shown in Eqs. (6)–(11) (Wang et al., 2014; Hou et al., 2018; Chen et al., 2021). The maximum allowable concentration of BrO₃⁻ produced by the reaction of SO₄^{•-} with Br⁻ in drinking water in China, the USA, and Europe is 10 µg/L (Delker et al., 2006; Guan et al., 2020). For ClO₃⁻, the health reference level recommended by the US EPA is 210 µg/L (Hou et al., 2018). Consequently, when use SR-AOPs for microbial inactivation, it is necessary to pay attention to the generated DBPs.





4.1 $SO_4^{\bullet-}$ and bromide

In the presence of $SO_4^{\bullet-}$, the conversion of Br^{-} to BrO_3^{-} is shown in Fig. 2 (Guan et al., 2020). Fang and Shang (2012) proposed that hypobromous acid/hypobromite ($HOBr/OBr^{-}$) are the key intermediates in the transformation processes from Br^{-} to BrO_3^{-} . The same phenomenon has also been found by other researchers (Li et al., 2015; Huang et al., 2017; Wen et al., 2018).

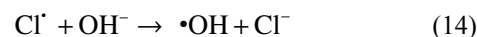
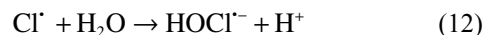
The formation of BrO_3^{-} is highly dependent on the reaction conditions. Wang et al. (2020b) and Huang et al. (2017) found that the more BrO_3^{-} is formed at high temperature. This may be because the high temperature facilitates the formation of $SO_4^{\bullet-}$, and therefore more BrO_3^{-} is formed.

NOM is another important factor that affects the formation of BrO_3^{-} . Many studies have proved that NOM has an inhibitory effect on the formation of BrO_3^{-} in SR-AOPs (Liu et al., 2018). For example, Fang and Shang (2012) found that in actual water bodies with NOM, the amount of BrO_3^{-} produced is lower than that in ultrapure water. But there is still controversy regarding the suppression mechanism in the presence of NOM. Fang and Shang (2012) believe that there are two main reasons why NOM inhibits the formation of bromate: 1) NOM reacted with the generated reactive bromine species; and 2) NOM reacted with the generated $SO_4^{\bullet-}$ (Fang and Shang, 2012; Yang et al., 2019). In contrast, Lutze et al. (2014) have different ideas. In their study, they observed that no organic brominated by-products were formed. Therefore, they proposed that the inhibition of BrO_3^{-} formation is ascribed to the reduction of $HOBr/OBr^{-}$ by the $O_2^{\bullet-}$ formed by the reaction of $SO_4^{\bullet-}$ with NOM. Liu et al. (2018) believed that the main reason why NOM inhibited the formation of BrO_3^{-} was the reaction between NOM and Br^{\bullet} , which converted Br^{\bullet} into Br^{-} . At the same time, they also believed that $O_2^{\bullet-}$ played an important role in inhibiting the generation of BrO_3^{-} . Interestingly, Lu et al. (2015) found organic bromination by-products, such as the formation of bromoacetic acid and bromoform, occurred in the study of bromide

transformation during thermally activated oxidation process of PS in the presence of HA. Moreover, they found that when the $SO_4^{\bullet-}$ at a low concentration, some of the bromine was present in organic forms such as brominated disinfection by-products (Br-DBPs). When the PS concentration exceeded 5 mmol/L, the organic brominated by-products formed would eventually be converted into bromate. Similar phenomena also appeared in the works of Wang et al. (2020b) and Liu et al. (2015). In addition, pH will also affect the formation of BrO_3^{-} . For example, Li et al. (2015) explored the generation of BrO_3^{-} in the Co^{2+}/PMS system at different pH values. They found that when the pH increased from 2.7 to 6.3, more bromate was formed. On the contrary, when the pH increased from 6.3 to 9.5, the BrO_3^{-} formed decreased. Besides NOM and pH, there are many other factors affecting the formation of BrO_3^{-} and Br-DBPs, which need to be further explored.

4.2 $SO_4^{\bullet-}$ and chlorine

Chloride is ubiquitous in the aqueous environment, thus $SO_4^{\bullet-}$ will inevitably react with Cl^{-} in the process of disinfection. During the reaction of $SO_4^{\bullet-}$ and Cl^{-} , chlorine atoms (Cl^{\bullet}) are produced as intermediate products. Lutze et al. (2015) confirmed that regardless of the presence or absence of external conditions such as NOM, model organic matter or bicarbonate, pH had a great influence on Cl^{\bullet} (Lutze et al., 2015; Ike et al., 2019). When the $pH < 5$, the Cl^{\bullet} was converted to ClO_3^{-} . But when the $pH > 5$, the Cl^{\bullet} mainly reacted with water to generate $\bullet OH$ (Eqs. (12)–(14)). It could be seen that under typical water treatment conditions of $pH > 6$, the formation of ClO_3^{-} could be ignored. Notably, they investigated that bicarbonate could scavenge Cl^{\bullet} and interrupted the conversion of $SO_4^{\bullet-}$ to $\bullet OH$.



Thus far, the way in which Cl^{-} is converted to ClO_3^{-} during SR-AOPs is unclear. But it may be similar to the way Br^{-} forms BrO_3^{-} . Hou et al. (2018) found that in both cobalt (II)/peroxymonosulfate (Co^{2+}/PMS) and UV/persulfate (UV/PS) systems, the generation of ClO_3^{-} was associated with the formation of hypochlorous acid/hypochlorite ($HOCl/OCl^{-}$). In the UV/PS system, they found that the generation of $HOCl/OCl^{-}$ and ClO_3^{-} was mainly

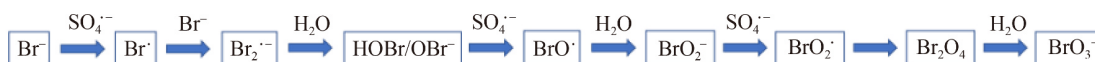
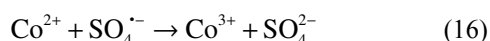
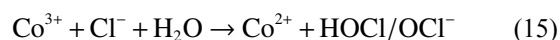


Fig. 2 Pathway of sulfate radical oxidation of Br^{-} to BrO_3^{-} (Guan et al., 2020) (Copyright 2020 Elsevier, Reprinted with permission from Elsevier).

attributed to $\text{SO}_4^{\bullet-}$. At the same time, they discovered that with the increase of Cl^- , more HOCl/OCl^- was produced, resulting in an increase in ClO_3^- production. However, the situation was slightly different in another system. In the Co/PMS system, Co^{3+} played an important role in the conversion of Cl^- into HOCl/OCl^- , and the formation of ClO_3^- was mainly ascribed to $\text{SO}_4^{\bullet-}$. At the same time, because of the high concentration of Cl^- accelerating the conversion of Co^{3+} to Co^{2+} (Eq. (15)), the generated Co^{2+} reacted with the $\text{SO}_4^{\bullet-}$ (Eq. (16)), resulting in the reduction of the $\text{SO}_4^{\bullet-}$, leading to the production of ClO_3^- increases first and then decreases.



Hua et al. (2019) systematically studied the DBPs formed by NOM and five model compounds after UV/ H_2O_2 , UV/PS treatment and 24 hours' chlorination treatment. They found that the effect of UV/ H_2O_2 treatment on the formation of DBPs was similar to that of UV/PS treatment, and the formation of DBPs after UV/ H_2O_2 treatment was higher than that of UV/PS treatment. The change of DBPs after UV/PS treatment mainly depended on the structure of the precursor and the water matrix. Different precursors and water matrix structures could produce different DBPs and had different effects on DBPs. For example, after UV/PS treatment, the trichloromethane (TCM) and chloral hydrate (CH) formed by benzoic acid (BA) increased significantly, while the TCM and CH formed by resorcinol decreased significantly. In addition, they also found that the presence of inorganic ions will affect the generation of DBPs. For instance, the presence of chloride and bicarbonate increases the generation of Cl-DBPs. And the presence of bromide reduces the formation of Cl-DBPs but increases the production of Br-DBPs. Chen et al. (2021) explored the generation of CX_3R -type DBPs in the process of cobalt-catalyzed peroxymonosulfate (Co^{2+} /PMS) oxidation. They found that Co^{3+} played a major role in the formation of CX_3R -type DBPs and the conversion of chlorine to chlorate was mainly due to $\text{SO}_4^{\bullet-}$. It was worth noting that it could simultaneously produce and degrade CX_3R -type DBPs. In the degradation process, both $\text{SO}_4^{\bullet-}$ and Co^{3+} could convert CX_3R -type DBPs into chlorides, in which $\text{SO}_4^{\bullet-}$ played a major role.

4.3 $\text{SO}_4^{\bullet-}$ and iodide

The standard reduction potential of iodide (I^-) is 1.33 V, which is more easily oxidized by $\text{SO}_4^{\bullet-}$ than Cl^- and Br^- (Wang et al., 2017b). The reactive iodine species (RIS) after the oxidation of I^- can also react with NOM to generate iodinated DBPs (I-DBPs) such as iodoacetic acid (IAAs) and iodoform, which can cause odor and taste

problems. Therefore, the formation of I-DBPs in the water disinfection process has been widely concerned. Wang et al. (2017b) used phenol to simulate NOM and investigated the conversion of I^- in the process of thermally activating PS. They discovered that I^- was converted into free iodine that attacks phenol, resulting in the formation of I-DBPs. Surprisingly, they observed that diiodoacetic acid (DIAA) was generated almost at the same time as iodophenol, and the generated DIAA was observably higher than triiodoacetic acid (TIAA), which was different from the traditional halogenation process. It indicated that there might be different ways of forming DIAA in this process. Contemporary, they also discovered that I-DBPs could react with excess $\text{SO}_4^{\bullet-}$ and converted to iodate (IO_3^-).

Hu et al. (2017) confirmed that pipe corrosion products (PCPs) can catalyze the degradation of iopamidol (IPM) by PMS. They found that most of I^- released from IPM was oxidized to IO_3^- , and a small part of the initial total organic iodine was converted to iodoform (CHI_3). And they also discovered that the water matrix would hinder the degradation of IPM. Similar conclusions were also proved in the degradation of IPM by the UV/PS system explored by Zhao et al. (2019b). The difference was that they noticed that $\text{SO}_4^{\bullet-}$ tended to oxidize the amino groups in IPM to nitro groups. At the same time, compared with the UV/ H_2O_2 and UV/NaClO systems, the UV/NaClO system had the least potential for the generation of I-DBPs.

4.4 $\text{SO}_4^{\bullet-}$ and organohalogens

The composition of the water matrix is very complex, in addition to bromine, chlorine and iodine, there are many halogenated organic pollutants. They can also react with $\text{SO}_4^{\bullet-}$ to form DBPs. The DBPs formed by the reaction of sulfate radicals with halogenated organic pollutants can not be ignored. For example, When using Co(II) to activate PMS to degrade tetrabromobisphenol A (TBBPA), Ji et al. (2016) found that although $\text{SO}_4^{\bullet-}$ can effectively degrade TBBPA, reactive intermediates such as reactive bromine species (RBS) and 2,4,6-tribromophenol (TBP) were formed. The formed intermediates could be further oxidized by RBS to Br-DBP such as bromoacetic acid and bromoform. Surprisingly, DBPs were mainly generated after TBBPA was degraded. The production of bromoform and monobromoacetic acid reached the maximum after 6 h and 10 h, which were 177.8 $\mu\text{g/L}$ and 38.4 $\mu\text{g/L}$, respectively. Afterwards, with the prolongation of the reaction time, the DBPs were degraded by $\text{SO}_4^{\bullet-}$ again.

When Xu et al. (2013) degraded 2,4,6-trichlorophenol (TCP) with Co^{2+} /PMS system, they found that the TCP degradation process would be accompanied by the generation of aromatic compounds such as 2,4,5-trichlorophenol and ring-opening products such as 2,4-

dichloro-5-oxygen-2-hexenoic acid. Anipsitakis et al. (2006) also found the formation of carbon tetrachloride in the same system. Zhao et al. (2019a) studied the degradation of iohexol in the Co^{2+} /PMS system under neutral conditions. The results showed that when 50 $\mu\text{mol/L}$ iohexol was degraded by 1 mmol/L PMS and 1 $\mu\text{mol/L}$ Co^{2+} , the CHI_3 and triiodoacetic acid produced within 12 h were 38.12 and 577.99 $\mu\text{g/L}$, respectively. Furthermore, the generation of I-DBP was significantly enhanced when HA was added. Hu et al. (2019a) also discovered the formation of CHI_3 when exploring the degradation of iohexol by the UV/PS system. The above works implies that attention should be paid to the generation of DBPs when using sulfate radicals to disinfect wastewater containing halogenated organic pollutants.

5 Future and challenge in $\text{SO}_4^{\cdot-}$ water disinfection techniques

In summary, the SR-AOPs technology has a very good inactivation efficiency for microorganisms. Compared with traditional water disinfection technology, it has broader application prospects. However, there are still many problems to be solved if the technology is applied in the actual disinfection process.

1) In the process of applying the SR-AOPs technology, its inactivation mechanism for microorganisms needs to be further explored. In various systems, it is necessary to explore the effect of experimental conditions such as the amount of disinfectant, temperature and pH on the inactivation efficiency. On this basis, the effect of actual water disinfection is explored. After that, pilot tests will be carried out to provide basis for large-scale application of this technology in practical water disinfection.

2) There are still many engineering challenges that must be solved before the full application of $\text{SO}_4^{\cdot-}$ water disinfection technology. For example, many metal catalysts and nano-material catalysts designed recent years have certain defects during the application process. Metal catalysts suffer from leakage of metal ions, and nanomaterial catalysts have the problem of high cost, which hinder their large-scale applications. Thus, in the actual application process, it is necessary to explore an efficient and economical activation method to increase the production of $\text{SO}_4^{\cdot-}$, so as to better inactivate microorganisms.

3) Before applying SR-AOPs for water disinfection treatment, the potential impact of this technology on the environment must be considered. If this method is used to disinfect water containing halogen ions such as Cl^- and Br^- , ClO_3^- and BrO_3^- will be generated. Meanwhile, when the water contains NOM, halogenated DBPs (such as Br-DBPs, Cl-DBPs and I-DBPs) will also be produced. Although compared with traditional disinfection

technology, the formation of DBPs is much less, but a certain amount of DBPs will still be produced. Therefore, it is necessary to further explore the formation of BrO_3^- , ClO_3^- , IO_3^- and halogenated DBPs in the actual water body and the influence of other environmental factors such as inorganic ions and pH on the formation of these DBPs.

In order to reduce the DBPs produced by SR-AOPs in the water disinfection process, it can be achieved by adjusting the pH of the water body and adding bicarbonate/carbonate. Studies have shown that when $\text{pH} > 5$, Cl^\bullet are more likely to be converted into $\bullet\text{OH}$, thereby reducing the production of ClO_3^- (Lutze et al., 2015). At the same time, there are reports that the higher the pH, the slower the conversion of Br^- to HOBr/BrO^- . Therefore, increasing pH can reduce the formation rate of XO_3^- (Fang and Shang, 2012). Since bicarbonate/carbonate can quench Cl^\bullet and their reaction rate with $\text{SO}_4^{\cdot-}$ is much slower than that of Cl^\bullet , bicarbonate/carbonate can be added into the system to reduce the formation of ClO_3^- (Mertens and von Sonntag, 1995). In addition, a novel catalyst can be developed to selectively remove XO_3^- and halogenated DBPs. It is also possible to introduce organic groups that can react with X^\bullet in the catalyst, thereby effectively inhibiting the formation of XO_3^- .

Besides, in the process of applying the SR-AOPs technology, the generated SO_4^{2-} is another potential hazard. SO_4^{2-} is harmless at low concentrations, but when the concentration exceeds the limit value, they are corrosive. Moreover, exposure to high concentrations of SO_4^{2-} in swimming pool water can cause various intestinal diseases when it enters the intestine. Therefore, the concentration of SO_4^{2-} can be reduced by ion exchange or the addition of lime (Bougie and Dubé, 2007). In addition, crystallization/precipitation techniques can also be used when the SO_4^{2-} concentration are excessive (Tait et al., 2009).

Acknowledgements The study was financially supported by the Project of the National Key Research and Development Program of China (No. 2021YFC1910404), the National Natural Science Foundation of China (Nos. 52100008, 52100184, and 52100142), the Funds of Hunan Science and Technology Innovation Project (China) (Nos. 2021GK4055 and 2022SK2119), Natural Science Foundation of Hunan Province, China (No. 2021JJ40091), the Science and Technology Innovation Program of Hunan Province (China) (No. 2021RC2056), and the Project funded by China Postdoctoral Science Foundation (No. 2021M701149).

Open Access This article is licensed under a Creative Commons Attribution 4.0 International License, which permits use, sharing, adaptation, distribution and reproduction in any medium or format, as long as you give appropriate credit to the original author(s) and the source, provide a link to the Creative Commons licence, and indicate if changes were made. The images or other third party material in this article are included in the article's Creative Commons licence, unless indicated otherwise in a credit line to the material. If material is not included in the article's Creative Commons licence and your intended use is not permitted by statutory regulation or exceeds the permitted use, you will need to obtain permission directly from the copyright holder. To view a copy of this

licence, visit <http://creativecommons.org/licenses/by/4.0/>.

References

- Anipsitakis G P, Dionysiou D D, Gonzalez M A (2006). Cobalt-mediated activation of peroxymonosulfate and sulfate radical attack on phenolic compounds: implications of chloride ions. *Environmental Science & Technology*, 40(3): 1000–1007
- Anipsitakis G P, Tufano T P, Dionysiou D D (2008). Chemical and microbial decontamination of pool water using activated potassium peroxymonosulfate. *Water Research*, 42(12): 2899–2910
- Ao X W, Eloranta J, Huang C H, Santoro D, Sun W J, Lu Z D, Li C (2021). Peracetic acid-based advanced oxidation processes for decontamination and disinfection of water: a review. *Water Research*, 188: 116479
- Bai L, Jiang Y, Xia D, Wei Z, Spinney R, Dionysiou D D, Minakata D, Xiao R, Xie H B, Chai L (2022). Mechanistic understanding of superoxide radical-mediated degradation of perfluorocarboxylic acids. *Environmental Science & Technology*, 56(1): 624–633
- Bianco A, Polo López M I, Fernández Ibáñez P, Brigante M, Mailhot G (2017). Disinfection of water inoculated with *Enterococcus faecalis* using solar/Fe(III)EDDS-H₂O₂ or S₂O₈²⁻ process. *Water Research*, 118: 249–260
- Bougie S, Dubé J (2007). Oxydation des isomères de dichlorobenzène à l'aide du persulfate de sodium soumis à une activation thermique. *Journal of Environmental Engineering & Science*, 6(4): 397–407(311)
- Chen T T, Yu Z Y, Xu T, Xiao R, Chu W H, Yin D Q (2021). Formation and degradation mechanisms of CX₃R-type oxidation by-products during cobalt catalyzed peroxymonosulfate oxidation: The roles of Co³⁺ and SO₄ center dot. *Journal of Hazardous Materials*, 405: 124243
- Cho M, Chung H, Choi W, Yoon J (2004). Linear correlation between inactivation of *E. coli* and OH radical concentration in TiO₂ photocatalytic disinfection. *Water Research*, 38(4): 1069–1077
- Davies M J, Gilbert B C, Norman R (1984). Electron spin resonance. Part 67: Oxidation of aliphatic sulphides and sulphoxides by the sulphate radical anion (SO₄⁻) and of aliphatic radicals by the peroxydisulphate anion (S₂O₈²⁻). *Journal of the Chemical Society, Perkin Transactions 2: Physical Organic Chemistry*, (3): 503–509
- Delker D, Hatch G, Allen J, Crissman B, George M, Geter D, Kilburn S, Moore T, Nelson G, Roop B, Slade R, Swank A, Ward W, DeAngelo A (2006). Molecular biomarkers of oxidative stress associated with bromate carcinogenicity. *Toxicology*, 221(2–3): 158–165
- Devasagayam T P A, Tilak J C, Bloor K K, Sane K S, Ghaskadbi S S, Lele R D (2004). Free radicals and antioxidants in human health: current status and future prospects. *Journal of the Association of Physicians of India*, 52: 794–804
- Fancy D A, Kodadek T (1999). Chemistry for the analysis of protein-protein interactions: rapid and efficient cross-linking triggered by long wavelength light. *Proceedings of the National Academy of Sciences of the United States of America*, 96(11): 6020–6024
- Fang J Y, Shang C (2012). Bromate formation from bromide oxidation by the UV/persulfate process. *Environmental Science & Technology*, 46(16): 8976–8983
- Ferreira L C, Castro-Alferez M, Nahim-Granados S, Polo-Lopez M I, Lucas M S, Li Puma G, Fernandez-Ibanez P (2020). Inactivation of water pathogens with solar photo-activated persulfate oxidation. *Chemical Engineering Journal*, 381: 122275
- Garkusheva N, Matafonova G, Tsenter I, Beck S, Batoev V, Linden K (2017). Simultaneous atrazine degradation and E-coli inactivation by simulated solar photo-Fenton-like process using persulfate. *Journal of Environmental Science and Health Part A: Toxic/Hazardous Substances & Environmental Engineering*, 52(9): 849–855
- Gau B C, Chen H, Zhang Y, Gross M L (2010). Sulfate radical anion as a new reagent for fast photochemical oxidation of proteins. *Analytical Chemistry*, 82(18): 7821–7827
- Ghanbari F, Moradi M (2017). Application of peroxymonosulfate and its activation methods for degradation of environmental organic pollutants. *Chemical Engineering Journal*, 310: 41–62
- Guan C, Jiang J, Pang S, Zhou Y, Gao Y, Li J, Wang Z (2020). Formation and control of bromate in sulfate radical-based oxidation processes for the treatment of waters containing bromide: a critical review. *Water Research*, 176: 115725
- Guerra-Rodriguez S, Rodriguez E, Singh D N, Rodriguez-Chueca J (2018). Assessment of sulfate radical-based advanced oxidation processes for water and wastewater treatment: a review. *Water*, 10(12): 1828
- Hou S D, Ling L, Dionysiou D D, Wan Y R, Huang J J, Guo K H, Li X C, Fang J Y (2018). Chlorate formation mechanism in the presence of sulfate radical, chloride, bromide and natural organic matter. *Environmental Science & Technology*, 52(11): 6317–6325
- Hu C Y, Hou Y Z, Lin Y L, Deng Y G, Hua S J, Du Y F, Chen C W, Wu C H (2019a). Kinetics and model development of iohexol degradation during UV/H₂O₂ and UV/S₂O₈²⁻ oxidation. *Chemosphere*, 229: 602–610
- Hu J, Dong H, Qu J, Qiang Z (2017). Enhanced degradation of iopamidol by peroxymonosulfate catalyzed by two pipe corrosion products (CuO and δ-MnO₂). *Water Research*, 112: 1–8
- Hu L, Wang P, Shen T, Wang Q, Wang X, Xu P, Zheng Q, Zhang G (2020). The application of microwaves in sulfate radical-based advanced oxidation processes for environmental remediation: a review. *Science of the Total Environment*, 722: 137831
- Hu P D, Long M C (2016). Cobalt-catalyzed sulfate radical-based advanced oxidation: A review on heterogeneous catalysts and applications. *Applied Catalysis B: Environmental*, 181: 103–117
- Hu Y R, Zhang T Y, Jiang L, Yao S J, Ye H, Lin K F, Cui C Z (2019b). Removal of sulfonamide antibiotic resistant bacterial and intracellular antibiotic resistance genes by UVC-activated peroxymonosulfate. *Chemical Engineering Journal*, 368: 888–895
- Hua Z, Kong X, Hou S, Zou S, Xu X, Huang H, Fang J (2019). DBP alteration from NOM and model compounds after UV/persulfate treatment with post chlorination. *Water Research*, 158: 237–245
- Huang X, Zhou X, Zhou J, Huang Z, Liu S, Qian G, Gao N (2017). Bromate inhibition by reduced graphene oxide in thermal/PMS process. *Water Research*, 122: 701–707
- Huie R E, Clifton C L (1993). Kinetics of the self-reaction of hydroxymethylperoxyl radicals. *Chemical Physics Letters*, 205(2–3): 163–167

- Ike I A, Karanfil T, Cho J, Hur J (2019). Oxidation byproducts from the degradation of dissolved organic matter by advanced oxidation processes - A critical review. *Water Research*, 164: 114929
- Ji Y, Kong D, Lu J, Jin H, Kang F, Yin X, Zhou Q (2016). Cobalt catalyzed peroxymonosulfate oxidation of tetrabromobisphenol A: kinetics, reaction pathways, and formation of brominated by-products. *Journal of Hazardous Materials*, 313: 229–237
- Lee H J, Kim H E, Kim M S, De Lannoy C F, Lee C (2020). Inactivation of bacterial planktonic cells and biofilms by Cu(II)-activated peroxymonosulfate in the presence of chloride ion. *Chemical Engineering Journal*, 380: 122468
- Lei X, Lei Y, Zhang X, Yang X (2021). Treating disinfection byproducts with UV or solar irradiation and in UV advanced oxidation processes: a review. *Journal of Hazardous Materials*, 408: 124435
- Lei Y, Chen C S, Tu Y J, Huang Y H, Zhang H (2015). Heterogeneous degradation of organic pollutants by persulfate activated by CuO-Fe₃O₄: mechanism, stability, and effects of pH and bicarbonate ions. *Environmental Science & Technology*, 49(11): 6838–6845
- Li Z, Chen Z, Xiang Y, Ling L, Fang J, Shang C, Dionysiou D D (2015). Bromate formation in bromide-containing water through the cobalt-mediated activation of peroxymonosulfate. *Water Research*, 83: 132–140
- Lian L, Yao B, Hou S, Fang J, Yan S, Song W (2017). Kinetic study of hydroxyl and sulfate radical-mediated oxidation of pharmaceuticals in wastewater effluents. *Environmental Science & Technology*, 51(5): 2954–2962
- Liang J H, Gao P, Li B H, Kang L F, Feng L, Han Q, Liu Y Z, Zhang L Q (2022). Characteristics of typical dissolved black carbons and their influence on the formation of disinfection by-products in chlor(am)ination. *Frontiers of Environmental Science & Engineering*, 16(12): 150
- Liu K, Bai L, Shi Y, Wei Z S, Spinney R, Goktas R K, Dionysiou D D, Xiao R Y (2020). Simultaneous disinfection of *E. faecalis* and degradation of carbamazepine by sulfate radicals: an experimental and modelling study. *Environmental Pollution*, 263: 114558
- Liu K, Lu J, Ji Y (2015). Formation of brominated disinfection by-products and bromate in cobalt catalyzed peroxymonosulfate oxidation of phenol. *Water Research*, 84: 1–7
- Liu Y Z, Yang Y, Pang S Y, Zhang L Q, Ma J, Luo C W, Guan C T, Jiang J (2018). Mechanistic insight into suppression of bromate formation by dissolved organic matters in sulfate radical-based advanced oxidation processes. *Chemical Engineering Journal*, 333: 200–205
- Lu J, Wu J, Ji Y, Kong D (2015). Transformation of bromide in thermo activated persulfate oxidation processes. *Water Research*, 78: 1–8
- Lutze H V, Bakkour R, Kerlin N, von Sonntag C, Schmidt T C (2014). Formation of bromate in sulfate radical based oxidation: mechanistic aspects and suppression by dissolved organic matter. *Water Research*, 53: 370–377
- Lutze H V, Kerlin N, Schmidt T C (2015). Sulfate radical-based water treatment in presence of chloride: formation of chlorate, interconversion of sulfate radicals into hydroxyl radicals and influence of bicarbonate. *Water Research*, 72: 349–360
- Ma H K, Zhang L L, Huang X M, Ding W, Jin H, Li Z F, Cheng S K, Zheng L (2019). A novel three-dimensional galvanic cell enhanced Fe²⁺/persulfate system: High efficiency, mechanism and damaging effect of antibiotic resistant E-coli and genes. *Chemical Engineering Journal*, 362: 667–678
- Marjanovic M, Giannakis S, Grandjean D, de Alencastro L F, Pulgarin C (2018). Effect of μM Fe addition, mild heat and solar UV on sulfate radical-mediated inactivation of bacteria, viruses, and micropollutant degradation in water. *Water Research*, 140: 220–231
- Mertens R, von Sonntag C (1995). Photolysis (λ = 354 nm) of tetrachloroethene in aqueous solutions. *Journal of Photochemistry and Photobiology A: Chemistry*, 85(1–2): 1–9
- Michael-Kordatou I, Iacovou M, Frontistis Z, Hapeshi E, Dionysiou D D, Fatta-Kassinos D (2015). Erythromycin oxidation and ERY-resistant *Escherichia coli* inactivation in urban wastewater by sulfate radical-based oxidation process under UV-C irradiation. *Water Research*, 85: 346–358
- Moreno-Andrés J, Farinango G, Romero-Martínez L, Acevedo-Merino A, Nebot E (2019). Application of persulfate salts for enhancing UV disinfection in marine waters. *Water Research*, 163: 114866
- Neta P, Huie R E, Ross A B (1988). Rate constants for reactions of inorganic radicals in aqueous solution. *Journal of Physical and Chemical Reference Data*, 17(3): 1027–1284
- Oh W D, Dong Z L, Lim T T (2016). Generation of sulfate radical through heterogeneous catalysis for organic contaminants removal: current development, challenges and prospects. *Applied Catalysis B: Environmental*, 194: 169–201
- Pignatello J J, Oliveros E, Mackay A (2006). Advanced oxidation processes for organic contaminant destruction based on the Fenton reaction and related chemistry. *Critical Reviews in Environmental Science and Technology*, 36(1): 1–84
- Qi W H, Zhu S M, Shitu A, Ye Z Y, Liu D Z (2020). Low concentration peroxymonosulfate and UVA-LED combination for *E. coli* inactivation and wastewater disinfection from recirculating aquaculture systems. *Journal of Water Process Engineering*, 36: 101362
- Richardson S D, Kimura S Y (2019). Water analysis: emerging contaminants and current issues. *Analytical Chemistry*, 92(1): 473–505
- Rodríguez-Chueca J, Barahona-García E, Blanco-Gutiérrez V, Isidoro-García L, Dos Santos-García A J (2020). Magnetic CoFe₂O₄ ferrite for peroxymonosulfate activation for disinfection of wastewater. *Chemical Engineering Journal*, 398: 125606
- Rodríguez-Chueca J, Giannakis S, Marjanovic M, Kohantorabi M, Gholami M R, Grandjean D, De Alencastro L F, Pulgarin C (2019a). Solar-assisted bacterial disinfection and removal of contaminants of emerging concern by Fe²⁺-activated HSO₅⁻ vs. S₂O₈²⁻ in drinking water. *Applied Catalysis B: Environmental*, 248: 62–72
- Rodríguez-Chueca J, Guerra-Rodríguez S, Ruez J M, Lopez-Munoz M J, Rodríguez E (2019b). Assessment of different iron species as activators of S₂O₈²⁻ and HSO₅⁻ for inactivation of wild bacteria strains. *Applied Catalysis B: Environmental*, 248: 54–61
- Rodríguez-Chueca J, Moreira S I, Lucas M S, Fernandes J R, Tavares P B, Sampaio A, Peres J A (2017a). Disinfection of simulated and real winery wastewater using sulphate radicals: peroxymonosulphate/transition metal/UV-A LED oxidation. *Journal of Cleaner Production*, 149: 805–817

- Rodríguez-Chueca J, Silva T, Fernandes J R, Lucas M S, Puma G L, Peres J A, Sampaio A (2017b). Inactivation of pathogenic microorganisms in freshwater using $\text{HSO}_5^-/\text{UV-A}$ LED and $\text{HSO}_5^-/\text{M}^{n+}/\text{UV-A}$ LED oxidation processes. *Water Research*, 123: 113–123
- Roginskaya M, Mohseni R, Ampadu-Boateng D, Razskazovskiy Y (2016). DNA damage by the sulfate radical anion: hydrogen abstraction from the sugar moiety versus one-electron oxidation of guanine. *Free Radical Research*, 50(7): 756–766
- Sabeti Z, Alimohammadi M, Yousefzadeh S, Aslani H, Ghani M, Nabizadeh R (2017). Application of response surface methodology for modeling and optimization of *Bacillus subtilis* spores inactivation by the UV/persulfate process. *Water Science and Technology: Water Supply*, 17(2): 342–351
- Shan H R, Si Y, Yu J Y, Ding B (2020). Flexible, mesoporous, and monodispersed metallic cobalt-embedded inorganic nanofibrous membranes enable ultra-fast and high-efficiency killing of bacteria. *Chemical Engineering Journal*, 382: 122909
- Sonntag C (2006). *Free-Radical-Induced DNA Damage and Its Repair: A Chemical Perspective*. Berlin: Springer Science & Business Media
- Subramanian G, Parakh P, Prakash H (2013). Photodegradation of methyl orange and photoinactivation of bacteria by visible light activation of persulphate using a tris(2,2'-bipyridyl)ruthenium(II) complex. *Photochemical & Photobiological Sciences*, 12(3): 456–466
- Sun P, Tyree C, Huang C H (2016). Inactivation of *Escherichia coli*, bacteriophage MS₂, and *Bacillus* spores under UV/H₂O₂ and UV/peroxydisulfate advanced disinfection conditions. *Environmental Science & Technology*, 50(8): 4448–4458
- Tait S, Clarke W P, Keller J, Batstone D J (2009). Removal of sulfate from high-strength wastewater by crystallisation. *Water Research*, 43(3): 762–772
- Tang J L, Wang J J, Tang L, Feng C Y, Zhu X, Yi Y Y, Feng H P, Yu J F, Ren X Y (2022). Preparation of floating porous g-C₃N₄ photocatalyst via a facile one-pot method for efficient photocatalytic elimination of tetracycline under visible light irradiation. *Chemical Engineering Journal*, 430: 132669
- Venieri D, Karapa A, Panagiotopoulou M, Gounaki I (2020). Application of activated persulfate for the inactivation of fecal bacterial indicators in water. *Journal of Environmental Management*, 261: 110223
- Waclawek S, Lutze H V, Grubel K, Padil V V T, Cernik M, Dionysiou D D (2017). Chemistry of persulfates in water and wastewater treatment: a review. *Chemical Engineering Journal*, 330: 44–62
- Waldemer R H, Tratnyek P G, Johnson R L, Nurmi J T (2007). Oxidation of chlorinated ethenes by heat-activated persulfate: kinetics and products. *Environmental Science & Technology*, 41(3): 1010–1015
- Wang H, Ma D F, Shi W Y, Yang Z Y, Cai Y, Gao B Y (2021). Formation of disinfection by-products during sodium hypochlorite cleaning of fouled membranes from membrane bioreactors. *Frontiers of Environmental Science & Engineering*, 15(5): 102
- Wang J, Chen H, Tang L, Zeng G, Liu Y, Yan M, Deng Y, Feng H, Yu J, Wang L (2018). Antibiotic removal from water: A highly efficient silver phosphate-based Z-scheme photocatalytic system under natural solar light. *Science of the Total Environment*, 639: 1462–1470
- Wang J J, Tang L, Zeng G M, Deng Y C, Liu Y N, Wang L G, Zhou Y Y, Guo Z, Wang J J, Zhang C (2017a). Atomic scale g-C₃N₄/Bi₂WO₆ 2D/2D heterojunction with enhanced photocatalytic degradation of ibuprofen under visible light irradiation. *Applied Catalysis B: Environmental*, 209: 285–294
- Wang J L, Wang S Z (2018). Activation of persulfate (PS) and peroxymonosulfate (PMS) and application for the degradation of emerging contaminants. *Chemical Engineering Journal*, 334: 1502–1517
- Wang L, Kong D, Ji Y, Lu J, Yin X, Zhou Q (2017b). Transformation of iodide and formation of iodinated by-products in heat activated persulfate oxidation process. *Chemosphere*, 181: 400–408
- Wang W, Wang H, Li G, An T, Zhao H, Wong P K (2019). Catalyst-free activation of persulfate by visible light for water disinfection: Efficiency and mechanisms. *Water Research*, 157: 106–118
- Wang W, Wang H, Li G, Wong P K, An T (2020a). Visible light activation of persulfate by magnetic hydrochar for bacterial inactivation: efficiency, recyclability and mechanisms. *Water Research*, 176: 115746
- Wang Y, Le Roux J, Zhang T, Croué J P (2014). Formation of brominated disinfection byproducts from natural organic matter isolates and model compounds in a sulfate radical-based oxidation process. *Environmental Science & Technology*, 48(24): 14534–14542
- Wang Z Y, Shao Y S, Gao N Y, Xu B, An N, Lu X (2020b). Comprehensive study on the formation of brominated byproducts during heat-activated persulfate degradation. *Chemical Engineering Journal*, 381: 122660
- Wen G, Qiang C, Feng Y B, Huang T L, Ma J (2018). Bromate formation during the oxidation of bromide-containing water by ozone/p peroxymonosulfate process: Influencing factors and mechanisms. *Chemical Engineering Journal*, 352: 316–324
- Wen G, Xu X Q, Zhu H, Huang T L, Ma J (2017). Inactivation of four genera of dominant fungal spores in groundwater using UV and UV/PMS: efficiency and mechanisms. *Chemical Engineering Journal*, 328: 619–628
- Wu X, Xu G, Zhu J J (2019). Sonochemical synthesis of Fe₃O₄/carbon nanotubes using low frequency ultrasonic devices and their performance for heterogeneous sono-persulfate process on inactivation of *Microcystis aeruginosa*. *Ultrasonics Sonochemistry*, 58: 104634
- Xia D, Li Y, Huang G, Yin R, An T, Li G, Zhao H, Lu A, Wong P K (2017). Activation of persulfates by natural magnetic pyrrhotite for water disinfection: efficiency, mechanisms, and stability. *Water Research*, 112: 236–247
- Xia D H, He H J W, Liu H D, Wang Y C, Zhang Q, Li Y, Lu A H, He C, Wong P K (2018). Persulfate-mediated catalytic and photocatalytic bacterial inactivation by magnetic natural ilmenite. *Applied Catalysis B: Environmental*, 238: 70–81
- Xia D H, Tang Z Y, Wang Y C, Yin R, He H J W, Xie X, Sun J L, He C, Wong P K, Zhang G (2020). Piezo-catalytic persulfate activation system for water advanced disinfection: process efficiency and inactivation mechanisms. *Chemical Engineering Journal*, 400: 125894

- Xiao R, Bai L, Liu K, Shi Y, Minakata D, Huang C H, Spinney R, Seth R, Dionysiou D D, Wei Z, Sun P (2020). Elucidating sulfate radical-mediated disinfection profiles and mechanisms of *Escherichia coli* and *Enterococcus faecalis* in municipal wastewater. *Water Research*, 173: 115552
- Xiao R Y, Liu K, Bai L, Minakata D, Seo Y, Göktaş R K, Dionysiou D D, Tang C J, Wei Z S, Spinney R (2019). Inactivation of pathogenic microorganisms by sulfate radical: present and future. *Chemical Engineering Journal*, 371: 222–232
- Xiao R Y, Luo Z H, Wei Z S, Luo S, Spinney R, Yang W C, Dionysiou D D (2018). Activation of peroxymonosulfate/persulfate by nanomaterials for sulfate radical-based advanced oxidation technologies. *Current Opinion in Chemical Engineering*, 19: 51–58
- Xie W, Dong W, Kong D, Ji Y, Lu J, Yin X (2016). Formation of halogenated disinfection by-products in cobalt-catalyzed peroxymonosulfate oxidation processes in the presence of halides. *Chemosphere*, 154: 613–619
- Xu L, Yuan R X, Guo Y G, Xiao D X, Cao Y, Wang Z H, Liu J S (2013). Sulfate radical-induced degradation of 2,4,6-trichlorophenol: a de novo formation of chlorinated compounds. *Chemical Engineering Journal*, 217: 169–173
- Yang J, Dong Z, Jiang C, Wang C, Liu H (2019). An overview of bromate formation in chemical oxidation processes: occurrence, mechanism, influencing factors, risk assessment, and control strategies. *Chemosphere*, 237: 124521
- Yang S, Wang P, Yang X, Shan L, Zhang W, Shao X, Niu R (2010). Degradation efficiencies of azo dye Acid Orange 7 by the interaction of heat, UV and anions with common oxidants: persulfate, peroxymonosulfate and hydrogen peroxide. *Journal of Hazardous Materials*, 179(1–3): 552–558
- Yu J F, Feng H P, Tang L, Pang Y, Zeng G M, Lu Y, Dong H R, Wang J J, Liu Y N, Feng C Y, Wang J J, Peng B, Ye S J (2020). Metal-free carbon materials for persulfate-based advanced oxidation process: microstructure, property and tailoring. *Progress in Materials Science*, 111: 100654
- Zhang A, Wang F, Chu W, Yang X, Pan Y, Zhu H (2019). Integrated control of CX₃R-type DBP formation by coupling thermally activated persulfate pre-oxidation and chloramination. *Water Research*, 160: 304–312
- Zhang C, Li Y, Wang C, Zheng X (2021). Different inactivation behaviors and mechanisms of representative pathogens (*Escherichia coli* bacteria, human adenoviruses and *Bacillus subtilis* spores) in g-C₃N₄-based metal-free visible-light-enabled photocatalytic disinfection. *Science of the Total Environment*, 755(Pt 1): 142588
- Zhang L L, Jin H, Ma H K, Gregory K, Qi Z W, Wang C X, Wu W T, Cang D Q, Li Z F (2020). Oxidative damage of antibiotic resistant *E. coli* and gene in a novel sulfidated micron zero-valent activated persulfate system. *Chemical Engineering Journal*, 381: 122787
- Zhang L S, Wong K H, Yip H Y, Hu C, Yu J C, Chan C Y, Wong P K (2010). Effective photocatalytic disinfection of *E. coli* K-12 using AgBr-Ag-Bi₂WO₆ nanojunction system irradiated by visible light: the role of diffusing hydroxyl radicals. *Environmental Science & Technology*, 44(4): 1392–1398
- Zhang Y, Zhou L, Zhang Y, Tan C (2014). Inactivation of *Bacillus subtilis* spores using various combinations of ultraviolet treatment with addition of hydrogen peroxide. *Photochemistry and Photobiology*, 90(3): 609–614
- Zhao H, Huang C H, Zhong C, Du P H, Sun P Z (2022). Enhanced formation of trihalomethane disinfection byproducts from halobenzoquinones under combined UV/chlorine conditions. *Frontiers of Environmental Science & Engineering*, 16(6): 76
- Zhao H X, Ji Y F, Kong D Y, Lu J H, Yin X M, Zhou Q S (2019a). Degradation of iohexol by Co²⁺ activated peroxymonosulfate oxidation: kinetics, reaction pathways, and formation of iodinated byproducts. *Chemical Engineering Journal*, 373: 1348–1356
- Zhao X, Jiang J, Pang S, Guan C, Li J, Wang Z, Ma J, Luo C (2019b). Degradation of iopamidol by three UV-based oxidation processes: kinetics, pathways, and formation of iodinated disinfection byproducts. *Chemosphere*, 221: 270–277
- Zhou S, Bu L, Shi Z, Deng L, Zhu S, Gao N (2018). Electrochemical inactivation of *Microcystis aeruginosa* using BDD electrodes: kinetic modeling of microcystins release and degradation. *Journal of Hazardous Materials*, 346: 73–81
- Zhou X, Yang Z Z, Chen Y, Feng H P, Yu J F, Tang J L, Ren X Y, Tang J, Wang J J, Tang L (2022). Single-atom Ru loaded on layered double hydroxide catalyzes peroxymonosulfate for effective *E. coli* inactivation via a non-radical pathway: efficiency and mechanism. *Journal of Hazardous Materials*, 440: 129720